*The AAPS Journal, Vol. 16, No. 4, July 2014 (© 2014)*
DOI: 10.1208/s12248-014-9593-8

*Research Article*

# Mechanistic Modeling of Monocarboxylate Transporter-Mediated Toxicokinetic/Toxicodynamic Interactions Between γ-Hydroxybutyrate and L-Lactate

**Bridget L. Morse,[1] Nisha Vijay,[1] and Marilyn E. Morris[1,2]**

*Received 3 January 2014; accepted 19 March 2014; published online 23 May 2014*

***Abstract*** Overdose of γ-hydroxybutyrate (GHB) can result in severe respiratory depression. Monocarboxylate transporter (MCT) inhibitors, including L-lactate, increase GHB clearance and represent a potential treatment for GHB intoxication. GHB can also affect L-lactate clearance, and L-lactate has been reported to affect respiration. In this research, we characterize these toxicokinetic/toxicodynamic interactions between GHB and L-lactate using mechanistic modeling. Plasma, urine, and respiration data were taken from our previous study in which GHB and sodium L-lactate were administered alone and concomitantly in rats. A model incorporating active renal reabsorption for both agents fit GHB and L-lactate toxicokinetic data. The $K_m$ for renal reabsorption of GHB (650 μg/mL) was close to its $K_m$ for the proton-dependent MCT1 and that for L-lactate (13.5 μg/mL) close to its $K_m$ for the sodium-dependent SMCT1. Inhibition of reabsorption by both agents was necessary to model concomitant drug administration. The metabolic $K_m$ for L-lactate closely resembled that for MCT-mediated hepatic uptake *in vitro*, and GHB inhibited this process. L-lactate significantly inhibited respiration at a high dose, and an indirect response model was used to fit these data. GHB toxicodynamics was modeled as a direct effect delayed by nonlinear transport into the brain extracellular fluid, with a $K_m$ value of 1,865 μg/mL for brain uptake which is similar to the *in vitro* $K_m$ value determined in rat brain endothelial cells. This model was useful for characterizing multiple MCT-mediated interactions. Incorporation of many parameters that can be determined *in vitro* may allow for clinical translation of these interactions.

**KEY WORDS:** γ-hydroxybutyrate; monocarboxylate transporter; toxicodynamics; toxicokinetics.

## INTRODUCTION

γ-Hydroxybutyrate (GHB) is a small chain fatty acid present endogenously *via* metabolism of γ-aminobutyric acid (GABA) in several human tissues, including the brain, where it acts as a neurotransmitter (1). Although originally developed for therapeutic use as a GABA analog, GHB has gained recent attention due to its abuse, with cases of overdose reported in several countries including the USA (2–4). Despite manifestations of GHB overdose including coma, respiratory depression, and death, there currently exists no clinically available treatment for GHB intoxication.

GHB is a substrate for a group of transporters known as the monocarboxylate transporters or MCTs (5,6). MCTs are proton-coupled transporters expressed highly and ubiquitously throughout the body, allowing them to govern many aspects of GHB toxicokinetics and indirectly its toxicodynamics. GHB toxicokinetics involves many dose-dependent processes in both rats and humans, including nonlinear absorption, metabolism, and renal clearance (7–9). Our laboratory previously demonstrated that in rats, the renal clearance of GHB increases with dose and that renal clearance could be increased with concomitant administration of MCT inhibitors, indicating the nonlinear renal clearance of GHB to be due to saturable MCT-mediated active renal reabsorption (7). *In situ* brain uptake studies demonstrated saturable transport of GHB, which could be inhibited by known MCT inhibitors, also suggesting a role of MCTs in GHB blood–brain barrier transport (10). We have also recently demonstrated inhibition of GHB blood–brain barrier transport in rats *in vivo* with MCT inhibition (11). In CaCo-2 cells, transport of GHB was found to be pH-dependent and also inhibited by MCT inhibitors, suggesting a role of MCTs in the oral absorption of GHB as well (12). Recent *in vivo* rat data also indicate increased oral clearance of GHB with MCT inhibitor administration and suggest effects of MCT inhibition on GHB absorption (13). Along with being a substrate of MCTs 1, 2, and 4 (SLC16A family), GHB is a substrate for the sodium-coupled SMCT1 (SLC5A8) (14), which is present in the kidney and intestine along with MCTs. This transporter may also play a role in GHB toxicokinetics and the effects of some MCT inhibitors on GHB transport in these tissues.

Due to the established ability of MCT inhibition to increase GHB elimination, administration of MCT inhibitors represents a potential therapeutic strategy for GHB overdose. Many of the aforementioned preclinical studies have assessed this potential using the MCT inhibitor L-lactate, as this inhibitor is clinically available in the form of sodium L-lactate for injection and Lactated Ringer's solution. We have also concluded in a clinical study that administration of L-lactate increases GHB renal clearance in humans (15). As a

[1] Department of Pharmaceutical Sciences, School of Pharmacy and Pharmaceutical Sciences, University at Buffalo, State University of New York, 352 Kapoor Hall, Buffalo, New York 14214-8033, USA.
[2] To whom correspondence should be addressed. (e–mail: memorris@buffalo.edu)

MCT and SMCT substrate, the pharmacokinetics of L-lactate is also governed by these transporters, and we found in a recent study that the concomitant administration of GHB and sodium L-lactate results in a dual toxicokinetic interaction in which each drug affects the clearance of the other (16). This study demonstrated improvement in GHB-induced respiratory depression by increasing GHB clearance with L-lactate administration, as well as by administration of $GABA_B$ receptor antagonists, as this receptor is responsible for respiratory depression and other toxicodynamic effects of GHB. Unlike L-lactate, however, $GABA_B$ receptor antagonists are not currently available for clinical use. In this previous study, we administered L-lactate to reach a clinically relevant increase in plasma lactate concentrations of 1.5 mM. As L-lactate has been noted to affect respiration, we evaluated the effect of this concentration of L-lactate alone on respiratory parameters and noted a slight, clinically insignificant respiratory inhibition. However, at higher concentrations in humans, sodium L-lactate infusions have elicited statistically and clinically significant inhibition of respiration (17). As one of the primary adverse effects and cause for fatality in GHB overdose is respiratory depression, understanding L-lactate effects on respiration is essential for its potential as a GHB overdose treatment option. In the current research, we sought to characterize the dose-dependent effects of sodium L-lactate on respiration in rats, as well as GHB effects, and the toxicokinetic/toxicodynamic interaction between the two agents using mechanistic modeling approaches.

## MATERIALS AND METHODS

### Chemicals and Reagents

GHB was provided by the National Institute on Drug Abuse (NIDA). Sodium L-lactate was purchased from Sigma Aldrich (St. Louis, MO). All other chemicals used were of analytical grade.

### Animals and Animal Surgery

Male Sprague–Dawley rats (Harlan Laboratories, Indianapolis, IN) weighing 270–330 g were used for the experiments. The animals were housed under controlled temperature and humidity with an artificial 12-h light/dark cycle, and food was available *ad libitum*. All animal protocols were approved by the Institutional Animal Care and Use Committee at the University at Buffalo. The animals were allowed to acclimate to their environment for a minimum of 1 week prior to surgical implantation of jugular and femoral vein cannulae under anesthesia with ketamine/xylazine. Cannulae were flushed daily with 40 IU/mL heparinized saline to maintain patency. The animals were allowed a minimum of 72 h for recovery from surgery before drug administration.

### Toxicokinetic/Toxicodynamic (TK/TD) Studies

Plasma, urine, and respiration data from rats administered GHB at IV doses of 200, 600, and 1,500 mg/kg; from animals administered sodium L-lactate at IV doses of 66 mg/kg+302.5 mg/kg/h or 605 mg/kg/h; and from animals administered GHB 1,500 mg/kg IV with IV sodium L-lactate 66 mg/kg+302.5 mg/kg/h were used from a previous study assessing GHB-induced respiratory depression (16). Further toxicokinetic/toxicodynamic data at a high dose of IV sodium L-lactate (198 mg/kg+1,210 mg/kg/h) as well as endogenous plasma lactate concentrations over time using a placebo group were obtained in the current study. A validation set of data was also created from animals administered GHB 600 mg/kg IV with IV sodium L-lactate 66 mg/kg+605 mg/kg/h. In the current and previous experiments, respiration was measured using plethysmography as previously described (16). Briefly, rats were placed in plethysmography chambers 1 h prior to drug administration and allowed a 45-min acclimation. Five baseline measurements were then taken over 15 min. GHB or L-lactate was then initiated after baseline measurements were obtained and considered time 0. For concomitant GHB and L-lactate administration, L-lactate was initiated at 5 min after GHB. Respiratory parameters of frequency (rate), tidal volume, and minute volume (frequency × tidal volume) were quantitated. GHB was administered as a 300-mg/mL bolus in sterile water *via* the jugular vein cannula. Sodium L-lactate bolus and infusion were administered as a 40-mg/mL solution in sterile water *via* the femoral vein cannula. L-lactate infusion continued for 8 h both alone and following GHB administration. Blood and urine were collected in all experiments.

### Sample Analysis

GHB plasma and urine concentrations were determined in rats administered GHB using previously described LC/MS/MS methods (16,18). Lactate plasma and urine concentrations were determined in all rats using a YSI Sport 1500 Lactate Analyzer (Yellow Springs Instruments, Yellow Springs, CO).

### TK/TD Model Structure

The toxicokinetic interaction model structure is given in Fig. 1, and the toxicodynamic model structure in Fig. 2. TK/TD model equations are given below. A description of each parameter is included in Table I. Models incorporating active renal reabsorption, as previously published for GHB (18), were used to fit GHB and lactate toxicokinetic data. Physiologic parameters were fixed to their physiologic values for rats of the same weight (18,19). A zero-order production rate ($k_{lac}$) was included in the lactate TK model to account for endogenous production of lactate. Endogenous production was not included for GHB as endogenous concentrations are negligible compared to those reached with exogenous GHB administration. Dashed lines in the model structure represent inhibitory functions. The effect of lactate on the active renal reabsorption of GHB was modeled assuming competitive inhibition, as was the effect of GHB on lactate renal reabsorption and on lactate metabolic clearance. A 1-h delay was incorporated to prevent effects of GHB on endogenous lactate prior to exogenous lactate reaching steady state at approximately 60 min, as discussed below. Toxicodynamic effect of GHB was modeled using a direct effect from GHB brain extracellular fluid (ECF) concentrations. As it is known that GHB blood–brain barrier transport is carrier-mediated, both influx and efflux transport kinetics for GHB brain distribution were incorporated into the model. The effect of GHB was modeled with inhibitory and stimulatory functions for frequency and tidal volume, respectively, and minute volume was modeled as the product of these two functions. Toxicodynamic effects of lactate were modeled using an indirect response model from plasma lactate concentrations with a linear stimulatory function on $k_{out}$ for both frequency and tidal volume (20).

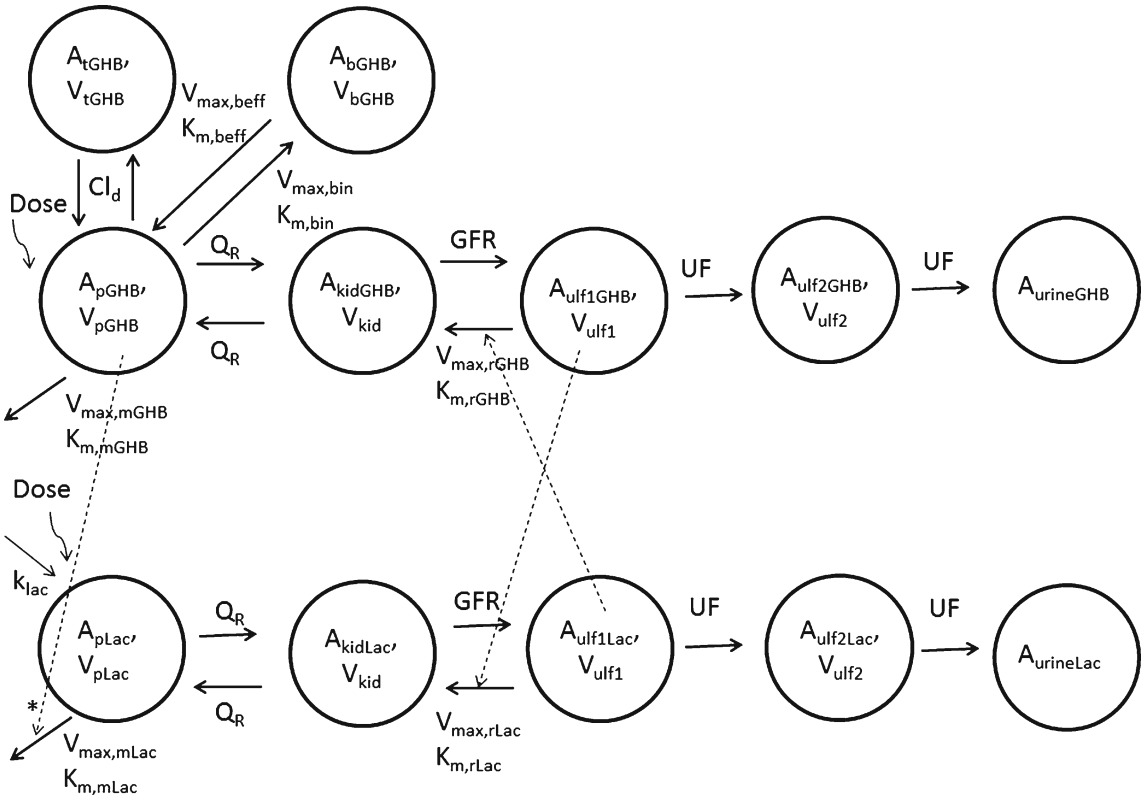


**Fig. 1.** Toxicokinetic interaction model structure. $A_X$ and $V_X$ represent the amount and volume respectively for X compartment. X=p=central, X=t=tissue, X=b=brain ECF, X=kid=kidney, X=ulf1=first ultrafiltrate compartment, X=ulf2=second ultrafiltrate compartment, X=urine=urine. $Q_R$ represents renal blood flow, *GFR* represents glomerular filtration rate, *UF* represents urine flow. $V_{max,m}$, $V_{max,r}$, $K_{m,m}$, and $K_{m,r}$ represent capacity and affinity constants for metabolism and renal reabsorption respectively. $V_{max,bin}$, $V_{max,beff}$, $K_{m,bin}$, and $K_{m,beff}$ represent capacity and affinity constants for transport of GHB into and out of the brain ECF. $k_{lac}$ represents endogenous production of lactate. *Dashed arrows* represent inhibitory functions. *Asterisk* a 1-h delay was incorporated for the inhibition of lactate metabolism by GHB

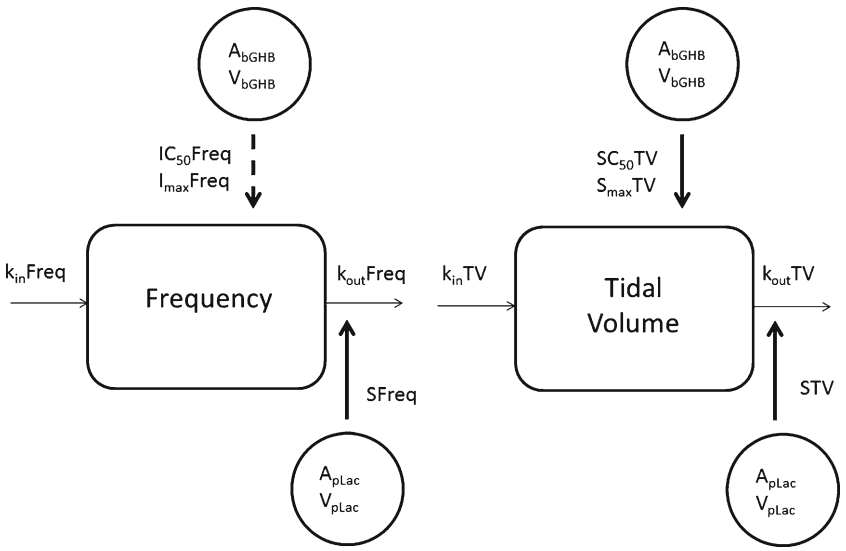


**Fig. 2.** Toxicodynamic model structure. $A_X$ and $V_X$ represent the amount and volume respectively for X compartment. *Solid arrows* represent stimulatory functions and *dashed arrows* inhibitory functions. *SFreq* and *STV* represent stimulatory constants for effect of lactate on $k_{out}$. $IC_{50}Freq$ and $I_{max}Freq$ represent inhibitory constants for GHB on frequency. $SC_{50}TV$ and $S_{max}TV$ represent stimulatory constants for GHB on tidal volume

Equations for lactate toxicokinetics:
If time <60 min, then:

$$dA_{\mathrm{pLac}}/dt = k_{\mathrm{lac}} - Q_R \cdot \frac{A_{\mathrm{pLac}}}{V_{\mathrm{pLac}}} + Q_R \cdot \frac{A_{\mathrm{kidLac}}}{V_{\mathrm{kid}}} - \frac{V_{\mathrm{max,mLac}}}{K_{\mathrm{m,mLac}} + \frac{A_{\mathrm{pLac}}}{V_{\mathrm{pLac}}}} \cdot \frac{A_{\mathrm{pLac}}}{V_{\mathrm{pLac}}}$$

If time ≥60 min, then:

$$dA_{\mathrm{pLac}}/dt = k_{\mathrm{lac}} - Q_R \cdot \frac{A_{\mathrm{pLac}}}{V_{\mathrm{pLac}}} + Q_R \cdot \frac{A_{\mathrm{kidLac}}}{V_{\mathrm{kid}}} - \frac{V_{\mathrm{max,mLac}}}{K_{\mathrm{m,mLac}} \cdot \left(1 + \frac{\frac{A_{\mathrm{pGHB}}}{V_{\mathrm{pGHB}}}}{K_{i,\mathrm{mGHB}}}\right) + \frac{A_{\mathrm{pLac}}}{V_{\mathrm{pLac}}}} \cdot \frac{A_{\mathrm{pLac}}}{V_{\mathrm{pLac}}}$$

$$dA_{\mathrm{kidLac}}/dt = Q_R \cdot \frac{A_{\mathrm{pLac}}}{V_{\mathrm{pLac}}} - (Q_R + \mathrm{GFR}) \cdot \frac{A_{\mathrm{kidLac}}}{V_{\mathrm{kid}}} + \frac{V_{\mathrm{max,rLac}}}{K_{\mathrm{m,rLac}} \cdot \left(1 + \frac{\frac{A_{\mathrm{ulf1GHB}}}{V_{\mathrm{ulf1}}}}{K_{i,\mathrm{rGHB}}}\right) + \frac{A_{\mathrm{ulf1Lac}}}{V_{\mathrm{ulf1}}}} \cdot \frac{A_{\mathrm{ulf1Lac}}}{V_{\mathrm{ulf1}}}$$

$$dA_{\mathrm{ulf1Lac}}/dt = \mathrm{GFR} \cdot \frac{A_{\mathrm{kidLac}}}{V_{\mathrm{kid}}} - \frac{V_{\mathrm{max,rLac}}}{K_{\mathrm{m,rLac}} \cdot \left(1 + \frac{\frac{A_{\mathrm{ulf1GHB}}}{V_{\mathrm{ulf1}}}}{K_{i,\mathrm{rGHB}}}\right) + \frac{A_{\mathrm{ulf1Lac}}}{V_{\mathrm{ulf1}}}} \cdot \frac{A_{\mathrm{ulf1GHB}}}{V_{\mathrm{ulf1}}} - \mathrm{UF} \cdot \frac{A_{\mathrm{ulf1Lac}}}{V_{\mathrm{ulf1}}}$$

$$dA_{\mathrm{ulf2Lac}}/dt = \mathrm{UF} \cdot \frac{A_{\mathrm{ulf1Lac}}}{V_{\mathrm{ulf1}}} - \mathrm{UF} \cdot \frac{A_{\mathrm{ulf2Lac}}}{V_{\mathrm{ulf2}}}$$

$$dA_{\mathrm{urineLac}}/dt = \mathrm{UF} \cdot \frac{A_{\mathrm{ulf2Lac}}}{V_{\mathrm{ulf2}}}$$

Equations for GHB toxicokinetics:

$$dA_{\mathrm{pGHB}}/dt = -(Q_R + Cl_{\mathrm{d}}) \cdot \frac{A_{\mathrm{pGHB}}}{V_{\mathrm{pGHB}}} + Cl_{\mathrm{d}} \cdot \frac{A_{\mathrm{tGHB}}}{V_{\mathrm{tGHB}}} + Q_R \cdot \frac{A_{\mathrm{kidGHB}}}{V_{\mathrm{kid}}} - \frac{V_{\mathrm{max,mGHB}}}{K_{\mathrm{m,mGHB}} + \frac{A_{\mathrm{pGHB}}}{V_{\mathrm{pGHB}}}} \cdot \frac{A_{\mathrm{pGHB}}}{V_{\mathrm{pGHB}}} - \frac{V_{\mathrm{max,binGHB}}}{K_{\mathrm{m,binGHB}} + \frac{A_{\mathrm{pGHB}}}{V_{\mathrm{pGHB}}}} \cdot \frac{A_{\mathrm{pGHB}}}{V_{\mathrm{pGHB}}} + \frac{V_{\mathrm{max,beffGHB}}}{K_{\mathrm{m,beffGHB}} + \frac{A_{\mathrm{bGHB}}}{V_{\mathrm{bGHB}}}} \cdot \frac{A_{\mathrm{bGHB}}}{V_{\mathrm{bGHB}}}$$

$$dA_{\mathrm{tGHB}}/dt = Cl_{\mathrm{d}} \cdot \frac{A_{\mathrm{pGHB}}}{V_{\mathrm{pGHB}}} - Cl_{\mathrm{d}} \cdot \frac{A_{\mathrm{tGHB}}}{V_{\mathrm{tGHB}}}$$

$$dA_{\mathrm{bGHB}}/dt = \frac{V_{\mathrm{max,binGHB}}}{K_{\mathrm{m,binGHB}} + \frac{A_{\mathrm{pGHB}}}{V_{\mathrm{pGHB}}}} \cdot \frac{A_{\mathrm{pGHB}}}{V_{\mathrm{pGHB}}} - \frac{V_{\mathrm{max,beffGHB}}}{K_{\mathrm{m,beffGHB}} + \frac{A_{\mathrm{bGHB}}}{V_{\mathrm{bGHB}}}} \cdot \frac{A_{\mathrm{bGHB}}}{V_{\mathrm{bGHB}}}$$

$$dA_{\mathrm{kidGHB}}/dt = Q_R \cdot \frac{A_{\mathrm{pGHB}}}{V_{\mathrm{pGHB}}} - (Q_R + \mathrm{GFR}) \cdot \frac{A_{\mathrm{kidGHB}}}{V_{\mathrm{kid}}} + \frac{V_{\mathrm{max,rGHB}}}{K_{\mathrm{m,rGHB}} \cdot \left(1 + \frac{\frac{A_{\mathrm{ulf1Lac}}}{V_{\mathrm{ulf1}}}}{K_{i,\mathrm{rLac}}}\right) + \frac{A_{\mathrm{ulf1GHB}}}{V_{\mathrm{ulf1}}}} \cdot \frac{A_{\mathrm{ulf1GHB}}}{V_{\mathrm{ulf1}}}$$

$$dA_{\mathrm{ulf1GHB}}/dt = \mathrm{GFR} \cdot \frac{A_{\mathrm{kidGHB}}}{V_{\mathrm{kid}}} - \frac{V_{\mathrm{max,rGHB}}}{K_{\mathrm{m,rGHB}} \cdot \left(1 + \frac{\frac{A_{\mathrm{ulf1Lac}}}{V_{\mathrm{ulf1}}}}{K_{i,\mathrm{rLac}}}\right) + \frac{A_{\mathrm{ulf1GHB}}}{V_{\mathrm{ulf1}}}} \cdot \frac{A_{\mathrm{ulf1GHB}}}{V_{\mathrm{ulf1}}} - UF \cdot \frac{A_{\mathrm{ulf1GHB}}}{V_{\mathrm{ulf1}}}$$

$$dA_{\mathrm{ulf2GHB}}/dt = \mathrm{UF} \cdot \frac{A_{\mathrm{ulf1GHB}}}{V_{\mathrm{ulf1}}} - \mathrm{UF} \cdot \frac{A_{\mathrm{ulf2GHB}}}{V_{\mathrm{ulf2}}}$$

$$dA_{\mathrm{urineGHB}}/dt = \mathrm{UF} \cdot \frac{A_{\mathrm{ulf2GHB}}}{V_{\mathrm{ulf2}}}$$

Equations for Lactate toxicodynamics:

$$d\mathrm{FrequencyLac}/dt = k_{\mathrm{in}}\mathrm{Freq} - k_{\mathrm{out}}\mathrm{Freq} \cdot \left\{1 + \left(\mathrm{Sfreq} \cdot \frac{A_{\mathrm{plac}}}{V_{\mathrm{plac}}}\right)\right\} \cdot \mathrm{Frequency}$$

$$d\mathrm{TidalVolumeLac}/dt = k_{\mathrm{in}}\mathrm{TV} - k_{\mathrm{out}}\mathrm{TV} \cdot \left\{1 + \left(\mathrm{STV} \cdot \frac{A_{\mathrm{plac}}}{V_{\mathrm{plac}}}\right)\right\} \cdot \mathrm{TV}$$

Equations for GHB toxicodynamics:

$$\mathrm{FrequencyGHB} = \mathrm{Freq0} \cdot \left\{1 - \left(\frac{\mathrm{Imax} \cdot \frac{A_{\mathrm{bGHB}}}{V_{\mathrm{bGHB}}}}{\mathrm{IC}_{50} + \frac{A_{\mathrm{bGHB}}}{V_{\mathrm{bGHB}}}}\right)\right\}$$

$$\text{Tidal VolumeGHB} = \text{TV0}\cdot\left\{1+\left(\frac{\text{Smax}\cdot\frac{A_{\text{bGHB}}}{V_{\text{bGHB}}}}{\text{SC}_{50}+\frac{A_{\text{bGHB}}}{V_{\text{bGHB}}}}\right)\right\}$$

Equations for GHB+L-lactate toxicodynamics:

$$\text{Frequency} = \text{FrequencyLac}-\text{Freq0}\cdot\left(\frac{\text{Imax}\cdot\frac{A_{\text{bGHB}}}{V_{\text{bGHB}}}}{IC_{50}+\frac{A_{\text{bGHB}}}{V_{\text{bGHB}}}}\right)$$

$$\text{Tidal Volume} = \text{TidalVolumeLac} + \text{TV0}\cdot\left(\frac{\text{Smax}\cdot\frac{A_{\text{bGHB}}}{V_{\text{bGHB}}}}{\text{SC}_{50}+\frac{A_{\text{bGHB}}}{V_{\text{bGHB}}}}\right)$$

### TK/TD Modeling and Simulation

All modelings were performed with ADAPT 5 software using the maximum likelihood function. Since GHB endogenous concentrations are negligible, TK/TD parameters for lactate could be determined alone without co-modeling with GHB. Since endogenous plasma lactate concentrations are not negligible and will therefore influence GHB toxicokinetics, GHB TK/TD parameters could only be determined by co-modeling with lactate. For this reason, L-lactate TK/TD data was modeled alone (using the above equations without competitive GHB inhibition), then these parameters fixed for the estimation of GHB TK/TD parameters and interaction parameters with the interaction model. Although both endogenous and exogenous lactates were presumed to affect GHB toxicokinetics, the effects of lactate on respiration were only included for exogenous sodium L-lactate administration, as effects are likely due to the sodium salt, as discussed below. Initial conditions for lactate plasma concentrations as well as initial conditions for toxicodynamic parameters for GHB and lactate were fixed to their known values. All other initial conditions were set to 0. The toxicokinetic model was used to fit plasma and urine data simultaneously. Output for plasma concentrations and urine amounts for both drugs were modeled as:

$$C_p = \frac{A_p}{V_p}$$

$$A_{\text{urine}} = A_{\text{urine}}$$

The variance model below was used with separate variance parameters for plasma, urine, frequency, and tidal volume estimated simultaneously with the TK/TD fitting:

$$\text{Var}(i) = (\sigma_1 + \sigma_2\cdot Y(i))^2$$

Standard goodness-of-fit criteria including Akaike Information Criterion, Schwarz Criterion, and coefficients of variance for model parameters were used to evaluate accurate description of the data. Following the identification of fitted model parameters, these parameters were fixed for simulation of TK/TD data for the GHB/sodium L-lactate dose combination given to the animals in the validation group.

### Data and Statistical Analysis

Lactate clearance (Cl) was calculated as Cl=infusion rate/$C_{ss}$ where $C_{ss}$ represents the mean steady-state concentration from 1 to 6 h after subtracting endogenous lactate concentrations. Percent urinary excretion was calculated as the total amount collected in the urine/total dose administered×100. One-way ANOVA followed by Tukey's *post hoc* test was used to determine statistically significant differences in lactate toxicokinetic parameters. Paired *t* tests were used to determine statistically significant differences in lactate toxicodynamics at 8 h compared to baseline. Unbound GHB brain ECF:plasma partition coefficients ($Kp_{u,u}$) were determined for each dose as $AUC_{\text{brainECF}}/AUC_{\text{plasma}}$ using simulated brain ECF concentrations and assuming negligible plasma protein binding of GHB, as demonstrated previously (7).

## RESULTS

### Lactate TK/TD

Lactate toxicokinetics and effects of sodium L-lactate administration alone on respiratory parameters are given in Table II. Lactate toxicokinetic and toxicodynamic profiles and model fittings are shown in Figs. 3 and 4. Resulting model parameters that were fixed for the interaction model are given in Table I. Total clearance of lactate decreased with increasing L-lactate infusion rates; therefore, plasma clearance of lactate was modeled with a nonlinear function. Inclusion of nonlinear clearance significantly improved the model fit, resulting in lower values for Akaike Information and Schwarz Criterion compared to a model with linear plasma clearance. Lactate volume of distribution was variable between groups and was not estimated by the model with acceptable precision. It was therefore fixed to a mean value of those calculated from each group using the initial concentration after bolus administration. Although renal elimination of lactate was very low at all doses, urinary excretion significantly increased at the highest dose, consistent with saturable renal reabsorption. Urinary lactate concentrations were undetectable without exogenous L-lactate administration. Administration of L-lactate at the two lower doses resulted in minimal decreases in both frequency and tidal volume, resulting in slight decreases in minute volume of 15–20%. The highest dose of L-lactate caused significant decreases in frequency and tidal volume, leading to a significant decrease in minute volume of ~30% compared to baseline. Toxicokinetic parameters determined for lactate were fixed to estimate the toxicodynamic parameters. Parameters for a nonlinear toxicodynamic effect could not be estimated with acceptable precision; therefore, a linear function was used to model lactate effects on both frequency and tidal volume.

### TK Interactions Between GHB and *l*-Lactate

GHB toxicokinetic and toxicodynamic profiles and fittings using the interaction model are shown in Figs. 5 and 6.

**Table I.** Model Parameters

| Parameter | Meaning | Value | CV% |
|---|---|---|---|
| Physiologic parameters | | | |
| $V_{kid}$ (mL) | Kidney volume | 4 | Fixed |
| $V_{ulf1}$ (mL) | Volume of 1st ultrafiltrate space | 3 | Fixed |
| $V_{ulf2}$ (mL) | Volume of 2nd ultrafiltrate space | 1 | Fixed |
| $Q_R$ (mL/min) | Renal blood flow | 12.5 | Fixed |
| GFR (mL/min) | Glomerular filtration rate | 3 | Fixed |
| UF (mL/min) | Urine flow | 0.1 | Fixed |
| $V_b$ (mL) | Volume of brain ECF | 0.35 | Fixed |
| Sodium L-lactate parameters | | | |
| $C_0$ (μg/mL) | Baseline lactate concentration | 188/184/174/172/192[a] | Fixed |
| $V_{pLac}$ (ml) | Lactate volume of central compartment | 278 | Fixed |
| $V_{max,mLac}$ (μg/min) | Lactate maximum metabolic rate | 1,470[b] | 4.8 |
| $K_{m,mLac}$ (μg/mL) | Lactate metabolic affinity constant | 256[b] | 32 |
| $V_{max,rLac}$ (μg/min) | Lactate maximum renal reabsorption rate | 1,550[b] | 4.6 |
| $K_{m,rLac}$ (μg/mL) | Lactate renal reabsorption affinity constant | 13.5[b] | 11 |
| $k_{lac}$(μg/min) | Endogenous lactate production rate | 4,970[b] | 24 |
| $k_{in}$Freq (breaths/min$^2$) | Baseline frequency input | 0.108[b] | 98 |
| $k_{out}$Freq (min$^{-1}$) | Baseline frequency output | 0.143E-02[b] | 80 |
| SFreq (mL/μg) | Slope of lactate effect on frequency | 0.119E-05[b] | 70 |
| $k_{in}$TV (breaths/min$^2$) | Baseline tidal volume input | 0.158E-02[b] | 29 |
| $k_{out}$TV (min$^{-1}$) | Baseline tidal volume output | 0.174E-02[b] | 25 |
| STV (mL/μg) | Slope of lactate effect on tidal volume | 0.105E-05[b] | 40 |
| GHB and interaction parameters | | | |
| $V_{pGHB}$ (mL) | GHB volume of central compartment | 88.5 | 12 |
| $Cl_{dGHB}$ (mL) | GHB tissue distribution clearance | 3.0 | 56 |
| $V_{tGHB}$ (mL) | GHB volume of tissue | 37.1 | 27 |
| $V_{max,mGHB}$ (μg/min) | GHB maximum metabolic rate | 889 | 7.0 |
| $K_{m,mGHB}$ (μg/mL) | GHB metabolic affinity constant | 130 | 17 |
| $V_{max,rGHB}$ (μg/min) | GHB maximum renal reabsorption rate | 2,808 | 7.8 |
| $K_{m,rGHB}$ (μg/mL) | GHB renal reabsorption affinity constant | 650 | 26 |
| $V_{max,binGHB}$ (μg/min) | GHB maximum brain uptake rate | 10.1 | 11 |
| $K_{max,binGHB}$ (μg/mL) | GHB brain uptake affinity constant | 1,853 | 39 |
| $V_{m,beffGHB}$ (μg/min) | GHB maximum brain efflux rate | 5.5 | 12 |
| $K_{m,beffGHB}$ (μg/mL) | GHB brain efflux affinity constant | 63 | 24 |
| $K_{i,rLac}$ (μg/mL) | Constant for inhibition of GHB renal reabsorption by lactate | 18.1 | 28 |
| $K_{i,rGHB}$ (μg/mL) | Constant for inhibition of lactate renal reabsorption by GHB | 318 | 6.8 |
| $K_{i,mGHB}$ (μg/mL) | Constant for inhibition of lactate metabolism by GHB | 398 | 15 |
| $IC_{50}$ and $SC_{50}$ (μg/mL) | Affinity constant for GHB on frequency and tidal volume | 82.8 | Fixed |
| $I_{max}$ | Maximum effect of GHB on frequency | 1.0 | Fixed |
| $S_{max}$ | Maximum effect of GHB on tidal volume | 3.0 | 3.3 |

*ECF* extracellular fluid, *CV%* coefficient of variation, *GHB* γ-hydroxybutyrate

[a] Fixed to known values for placebo, low, medium, and high doses of sodium L-lactate alone, and low sodium L-lactate+GHB groups respectively

[b] Fixed for the determination of GHB and interaction parameters

Toxicokinetic profiles and fittings for lactate data in the presence of GHB are shown in Fig. 7. Resulting model parameters are given in Table II. As previously reported (18), the toxicodynamic model incorporating active renal reabsorption was able to describe well the nonlinear renal clearance of GHB, with the percent GHB excreted in the urine ranging from 6 to 60% at the current dose range. A simple linear biophase model was initially tried in fitting the GHB toxicodynamic data, but was unable to capture this delayed effect at the highest dose. However, as observed in Fig. 6, incorporation of nonlinear transport into the brain allowed the model to capture the delay in the maximum effect at the highest GHB dose, compared to the two lower doses, with only the highest dose reaching plasma concentrations above the $K_m$ value for brain uptake. Fixing the $IC_{50}$ and $SC_{50}$ for frequency and tidal volume to a reported value for GHB binding to the $GABA_B$ receptor (21) allowed the model to also capture efflux transport parameters and for simulation of GHB brain ECF concentrations. As shown by the simulated GHB brain ECF concentrations in Fig. 5, fixing these values also allowed the brain ECF:plasma $Kp_{u,u}$ value to be less than one at values of 0.08–0.13 for each dose, which is very similar to the values experimentally determined for GHB using microdialysis (19,22). Although brain microdialysis data exist for GHB, these data were not used in the current model, as they were obtained in the striatum and frontal cortex, whereas the effects of GHB on respiration are presumed to occur in the brain stem. However, data at both sites agree with a low $Kp_{u,u}$ value for GHB brain partitioning predicted by the current model. $I_{max}$ for the effect of GHB on respiratory frequency was also fixed to 1, as it is known

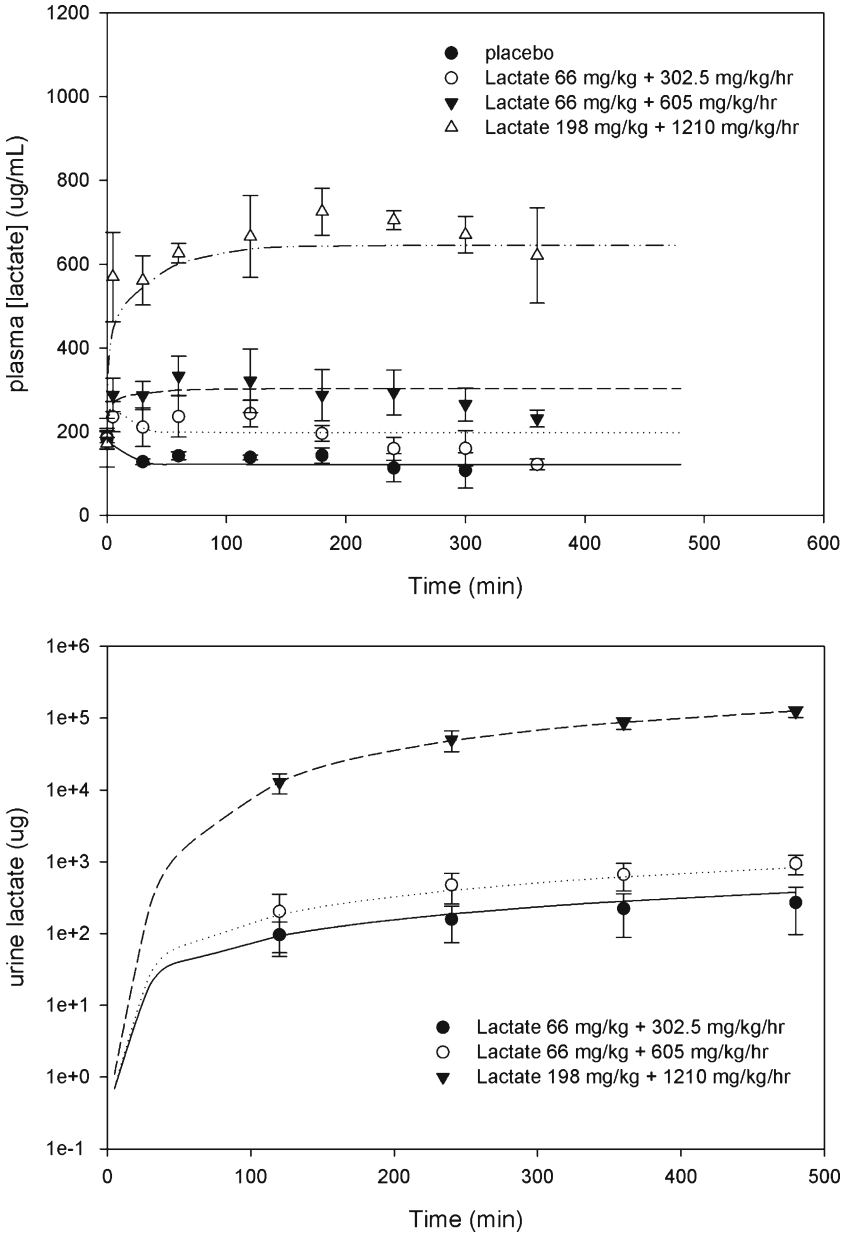


**Fig. 3.** Lactate toxicokinetics. Sodium L-lactate was administered intravenously at time 0 at the three doses indicated. Infusions were continued for 8 h over which plasma, urine, and respiratory measurements were obtained. Endogenous lactate concentrations were obtained in the placebo group administered normal saline. *Symbols* represent data collected and *lines* represent model fittings. Data presented as mean±SD, $n$=3–5

that GHB can cause complete respiratory arrest. Competitive inhibition by GHB on the metabolic clearance of lactate was necessary to capture the increase in lactate concentrations with concomitant drug administration, although interestingly, GHB did not have this effect on endogenous lactate concentrations as seen in Fig. 7. For this reason, the inhibition function was only added during exogenous lactate administration, and a time delay was also incorporated so that GHB did not have any effect on endogenous lactate concentrations prior to exogenous lactate reaching steady state. Incorporation of simultaneous competitive inhibition on active renal reabsorption captured the increased renal elimination of both drugs when given concomitantly and led to the associated decrease in GHB plasma concentrations. Simulation of the validation set of data overlays the experimental data well and indicates good predictive ability of the model using a dose combination outside those used in the fitting of model parameters (Fig. 8).

## DISCUSSION

While GHB abuse remains a significant issue in public health, there still exists no pharmacologic treatment for GHB overdose. MCT inhibition represents a potential safe,

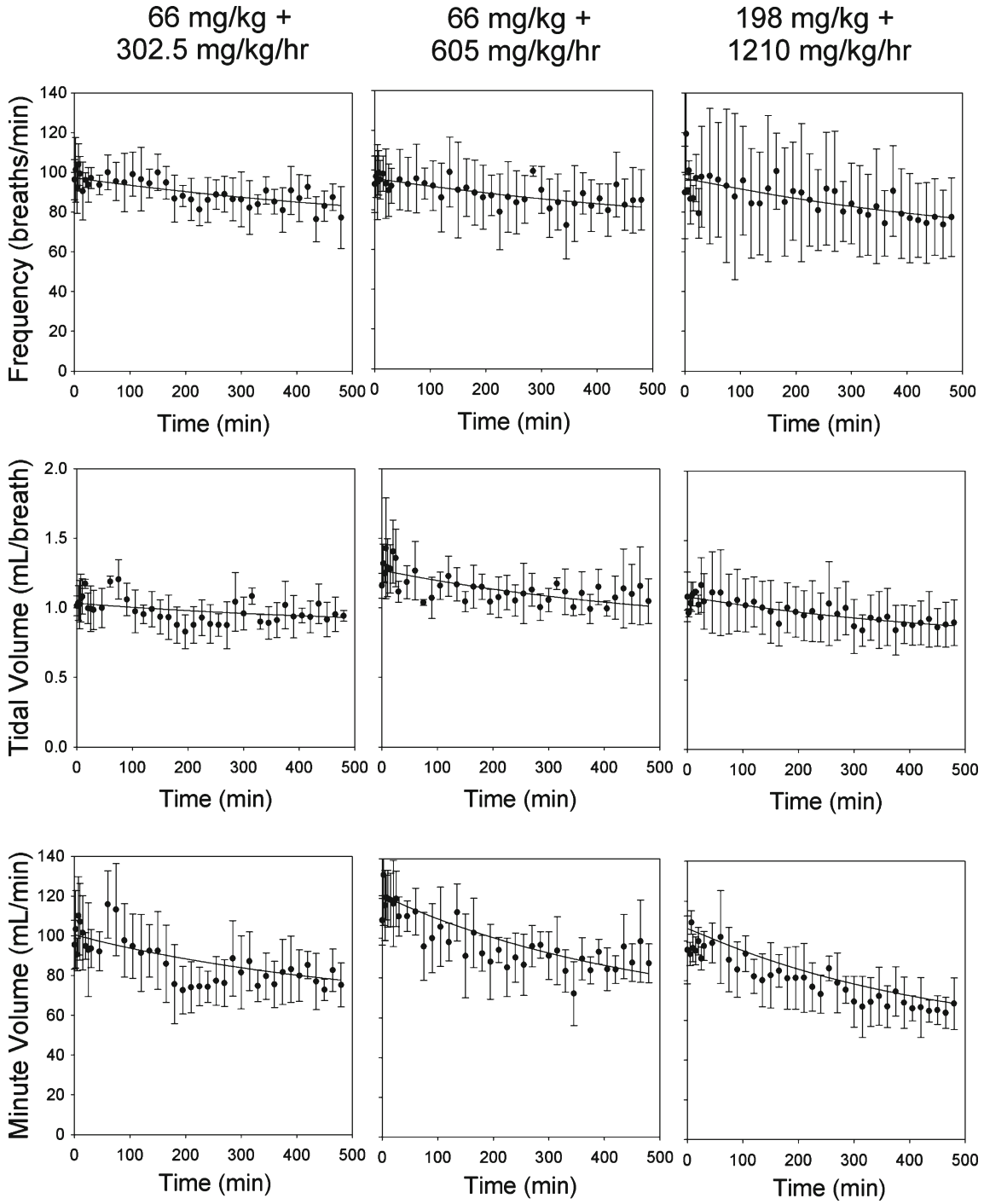


**Fig. 4.** Lactate toxicodynamics. Sodium L-lactate was administered intravenously at time 0 at the three doses indicated. Infusions were continued for 8 h over which time plasma, urine, and respiratory measurements were obtained. *Symbols* represent data collected and *lines* represent model fittings. Data presented as mean±SD, $n$=3–5

effective, and clinically available treatment option. Quantitative analysis of GHB TK/TD including the role of MCTs using mechanistic modeling aids in the understanding of GHB effects in overdose as well as the potential of MCT inhibition as an overdose treatment. Additionally, other therapeutic agents including statins, valproic acid, and NSAIDs have been demonstrated to interact with MCTs (23); therefore, an understanding of the role of MCTs in drug distribution and drug interactions may apply to other clinical situations.

In the current research, we characterize the TK/TD of GHB and lactate incorporating MCT-mediated transport at multiple physiologic sites. Both GHB and lactate toxicokinetics could be described by incorporating active renal reabsorption. Even though renal elimination of lactate was negligible at all doses evaluated, the incorporation of lactate urine data allowed the determination of lactate renal reabsorptive parameters in the renal tubule, a site of interest for the GHB/lactate interaction. The high-affinity renal $K_m$

**Table II.** Toxicokinetics/Toxicodynamics of Sodium L-Lactate

| Dose | Cl (ml/kg/min) | Urinary excretion (%) | Baseline frequency | 8 h frequency | Baseline tidal volume | 8 h tidal volume | Baseline minute volume | 8 h minute volume |
|---|---|---|---|---|---|---|---|---|
| 66 mg/kg+302.5 mg/kg/h | 91.1 (30) | 0.05 (0.02) | 93 (6) | 84 (7) | 1.01 (0.29) | 0.96 (0.081) | 92.9 (6.7) | 78.9 (6.2)* |
| 66 mg/kg+605 mg/kg/h | 65.0 (15)# | 0.07 (0.02) | 92 (13) | 86 (15)* | 1.16 (0.048) | 1.10 (0.18) | 108 (14) | 90.7 (7.3) |
| 198 mg/kg+1210 mg/kg/h | 37.1 (2.1)# | 4.2 (0.7)# | 91 (20) | 77 (18)* | 1.06 (0.13) | 0.909 (0.14)** | 93.8 (14) | 67.1 (10)** |

The three doses of L-lactate were each administered for 8 h during which plasma, urine, and respiratory measurements were collected ($n$=3–5/group). Data presented as mean (SD)
# $P<0.05$ (significantly different from L-lactate 302.5 mg/kg/h); *$P<0.05$ (significantly different from baseline); **$P<0.01$ (significantly different from baseline)

value for lactate of 13.5 μg/mL (150 μM) reflects this low renal excretion, and this value is similar to values reported for SMCT1-mediated transport of lactate (24), suggesting this transporter is primarily involved in lactate reabsorption. This is in agreement with studies in $SMCT^{-/-}$ mice in which 67-fold higher urinary lactate concentrations were observed compared to wild-type mice (25). On the other hand, the lower affinity renal $K_m$ value for GHB of 650 μg/mL (6.25 mM) is similar to that determined for rat MCT1 *in vitro* of 478 μg/mL (4.6 mM) as well as in rat brush-border membrane vesicles of 832 μg/mL (8.0 mM) determined at relevant urinary pH values (5). Interestingly, although the $K_m$ value for GHB suggests MCT-mediated renal reabsorption, the $K_i$ value for the inhibition of GHB renal reabsorption by lactate of 18.1 μg/mL (201 μM) is close to the $IC_{50}$ value determined previously for inhibition of SMCT-mediated GHB transport by L-lactate of 101 μM. This suggests the effects of L-lactate on GHB renal reabsorption to be mediated primarily by SMCT1 even though this may not be the primary transporter involved in the renal reabsorption of GHB. L-Lactate administration increased GHB renal clearance by ~30% in these experiments from 3.18 to 4.22 mL/kg/min (16). Even with L-lactate administration, the renal clearance of GHB is still far below that of the glomerular filtration rate in rats (~10 mL/kg/min; 7), indicating a considerable GHB renal reabsorption still occurs with L-lactate administration, which is consistent with the inhibition of a transporter other than that primarily responsible for GHB renal reabsorption. It is likely that more potent inhibitors of MCT1 may be more effective at inhibiting GHB renal reabsorption, some of which are currently in development (26).

Along with nonlinear renal clearance, nonlinear plasma clearance of GHB has been well-described, and the current metabolic $K_m$ value of 130 μg/mL is within the range of 54–579 μg/mL, as reported in other modeling efforts (8,18,19). However, an interesting finding in the current study was nonlinearity in the metabolic clearance of lactate. The $K_m$ value for this process of 256 μg/mL (2.84 mM) is very similar to the value determined in rat hepatocytes *in vitro* at pH 7.4 of 2.42 mM as well as that for MCT1 of 2.2 mM (27,28), suggesting that this nonlinearity is due to MCT-mediated uptake–rate limited hepatic elimination of lactate. Rat liver perfusion studies also suggest lactate hepatic metabolism to be uptake–rate limited (29).

The toxicokinetic interaction between GHB and lactate is interesting in that one increases while one decreases the clearance of the other even though both are substrates for the same transporters. The differences in the degree of renal reabsorption, as well as the differences in plasma concentrations of each agent can likely explain these effects. While renal excretion of L-lactate is negligible at all evaluated doses, renal elimination significantly contributes to GHB clearance at the high plasma concentrations obtained in this study. Therefore, while each drug decreases the other's renal reabsorption based upon the current data, an effect of increased plasma clearance with increased renal clearance is only observed with GHB. Additionally, while MCTs may be involved in the hepatic uptake of both agents prior to metabolism, the plasma concentrations of GHB in this study reach 40 mM, while the highest plasma lactate concentrations are below 8 mM. The 5-fold higher GHB concentrations likely explain why GHB decreases lactate metabolism/hepatic uptake and not *vice versa*. Furthermore, the effect of L-lactate on GHB renal clearance likely involves SMCT1, which is expressed in the kidney but not in the liver, also potentially explaining the effect of lactate on GHB renal but not hepatic clearance. Another interesting effect of this interaction is the inhibition of exogenous, but not endogenous, lactate metabolism by GHB. As bi-directional transporters, MCT-mediated drug–drug interactions are less predictable, as additional substrate may inhibit uptake, inhibit efflux, or cause transstimulation of endogenous substrate. It is likely that a combination of these processes is involved in the complex interaction observed; however, currently, we cannot clearly define the mechanism behind this phenomenon.

As mentioned, the brain uptake of GHB is also MCT-mediated, and the brain distribution of GHB can be affected by L-lactate administration (11). A previous study using microdialysis demonstrated that the current dose of L-lactate had no effect on GHB brain distribution, although higher doses significantly decreased the brain:plasma ratio (11). For this reason, inhibition of GHB brain uptake by lactate was not incorporated in this model; however, the delay in GHB maximum effect could be attributed to this carrier-mediated process. Indeed, the $K_{m,bin}$ value of 1,853 μg/mL (17.8 mM) for GHB brain uptake that was achieved with this model is very similar to the value of 23.3 mM that we have observed in a rat brain endothelial cell line at pH 7.4 (22). This value is also similar to the value of 17.1 mM determined for GHB transport by MCT1 in red blood cells at pH 7.4 (30), suggesting this model is capturing the MCT1-mediated brain uptake parameters for GHB. Although the transport of GHB in the kidney and in the brain may both primarily involve

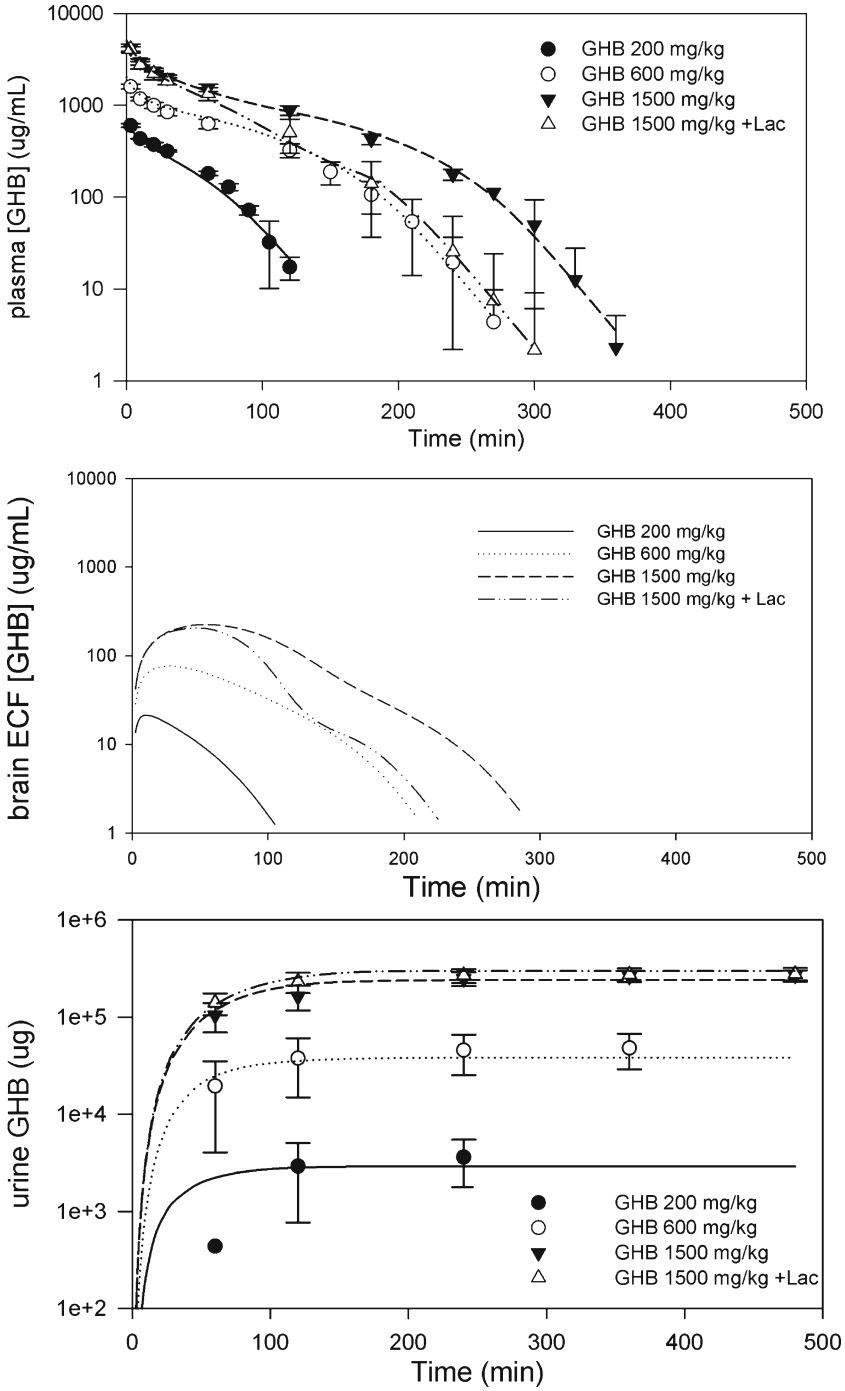


**Fig. 5.** GHB toxicokinetics with and without L-lactate administration. GHB was administered intravenously at time 0 at doses of 200, 600, and 1,500 mg/kg. For concomitant GHB/L-lactate administration, GHB 1,500 mg/kg was administered intravenously at time 0, and intravenous sodium L-lactate was initiated 5 min after GHB at a dose of 66 mg/kg+302.5 mg/kg/h for 8 h. In all experiments, plasma and urine were collected for up to 8 h. Respiratory measurements were also collected for 8 h in all experiments. *Symbols* represent data collected and *lines* represent model fittings for plasma and urine data. GHB brain ECF concentrations were simulated for each dose using the fitted model parameters. Data presented as mean±SD, $n$=4–6

MCT1, we previously demonstrated that the $K_m$ and $V_{max}$ values for GHB MCT1-mediated transport change with pH at the transport site; therefore, different values are expected for transport at these two physiologic sites due to different physiologic pH, a difference also captured with this model. While the clinical relevance of saturable brain transport has been brought into question due to typically lower plasma drug concentrations in humans (31), situations concerning drug overdoses such as that of GHB are likely unique in this respect. With our current rat data, GHB concentrations range

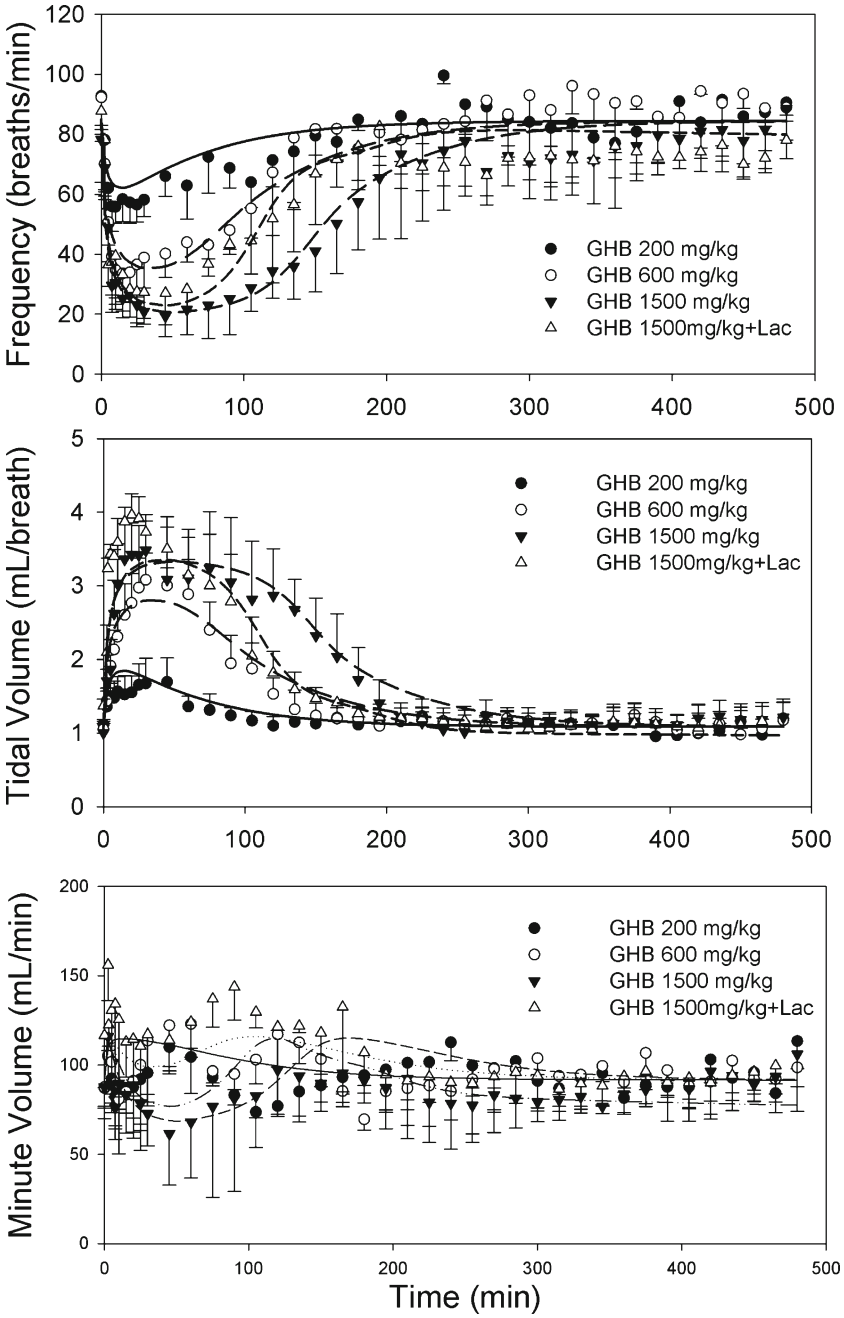


**Fig. 6.** GHB toxicodynamics with and without L-lactate administration. GHB was administered intravenously at time 0 at doses of 200, 600, and 1,500 mg/kg. For concomitant GHB/L-lactate administration, GHB 1,500 mg/kg was administered intravenously at time 0, and intravenous sodium L-lactate was initiated 5 min after GHB at a dose of 66 mg/kg+302.5 mg/kg/h for 8 h. Respiratory measurements were collected for 8 h in all experiments. Plasma and urine were also collected in all experiments. *Symbols* represent data collected and *lines* represent model fittings. Data presented as mean±SD, $n$=4–6

from approximately 1 to 4,000 μg/mL. In clinical cases of GHB overdoses, concentrations even exceeding 4,000 μg/mL have been reported (3). Assuming similar $K_m$ and $Kp_{u,u}$ values between species, it is likely that GHB plasma and brain concentrations will exceed $K_m$ values for uptake and/or efflux in GHB intoxication. Additionally, it should be noted that GHB has negligible protein binding in plasma (7).

A potentially very useful aspect of the current model is that it was able to accurately predict the brain ECF:plasma $Kp_{u,u}$ value using brain uptake, brain efflux, and receptor-binding parameters, all of which can be determined *in vitro* without the need for actual brain ECF concentration profiles. This may highly aid in the translational ability of the model to accurately simulate clinical effects of GHB in the brain without the availability of human brain concentrations. However, while this model was able to capture influx and efflux parameters for GHB transport in the brain, efflux may not be the only route of GHB brain elimination. Our

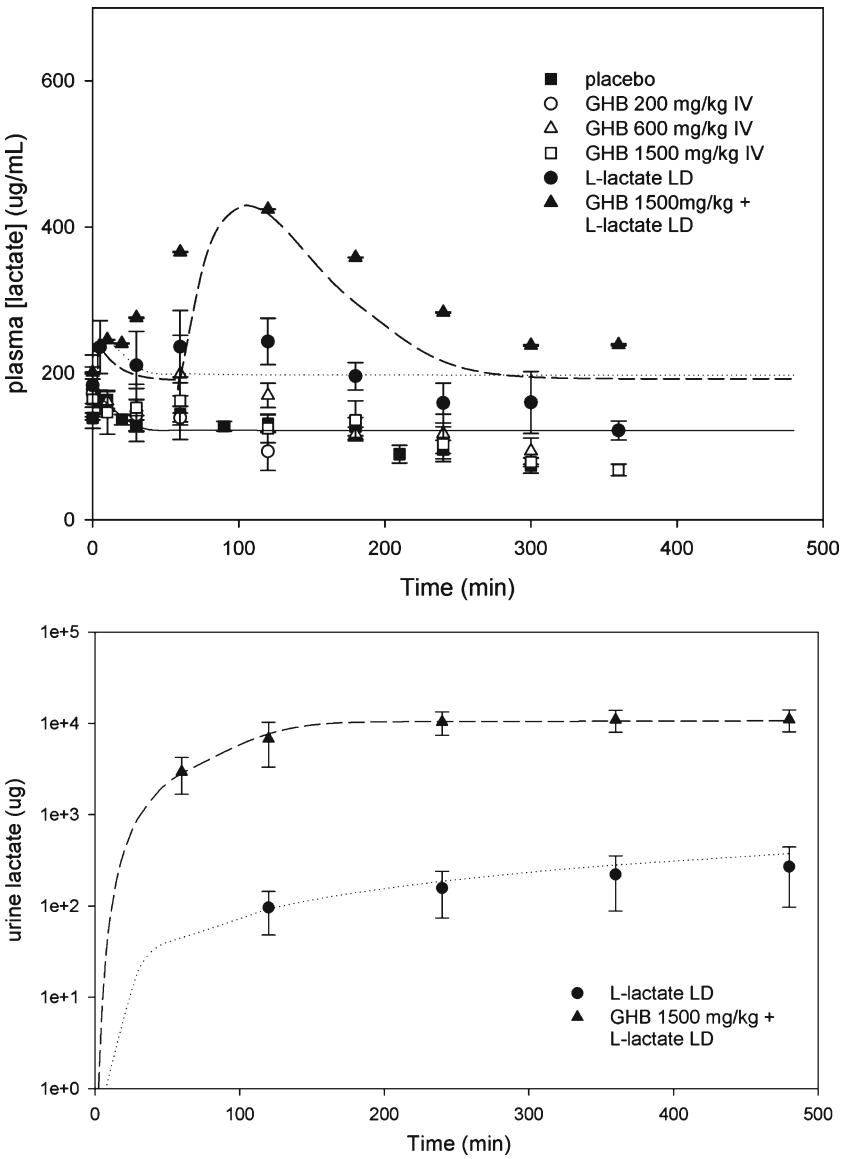


**Fig. 7.** Lactate toxicokinetics in the presence and absence of GHB. L-Lactate LD=66 mg/kg+302.5 mg/kg/h. For GHB administered alone, GHB was given intravenously at time 0 at doses of 200, 600, and 1,500 mg/kg. For administration of L-lactate LD alone, a sodium L-lactate intravenous bolus and infusion were initiated at time 0 and continued for 8 h. For concomitant drug administration, GHB 1,500 mg/kg was administered intravenously at time 0, and intravenous sodium L-lactate was initiated 5 min after GHB and continued for 8 h. The placebo group received an intravenous bolus of normal saline. *Symbols* represent data collected and *dashed lines* represent model fittings. *Solid and dotted lines* represent simulations for endogenous and L-lactate LD alone, respectively, using TK parameters for lactate alone that were fixed in the interaction model. Data presented as mean±SD, $n$=4–6

laboratory has evaluated brain metabolism of GHB *in vitro* and observed no degradation, indicating brain metabolism to be a negligible elimination pathway (unpublished data); however, we have previously detected GHB in cerebrospinal fluid in rats (32), indicating GHB may be removed by bulk flow along with blood–brain barrier efflux. However, in a previous effort to model GHB plasma concentrations along with simultaneously collected brain ECF concentrations, both plasma and ECF concentration profiles were well-described using a model including only brain efflux directly back into the plasma without the delayed re-entrance into the plasma through the CSF (19). Furthermore, we have evaluated GHB efflux in rat brain endothelial cells (11), observing efficient efflux, with approximately 10% of GHB remaining intracellularly at steady state compared to that at initial incubation. This efflux could also be trans-stimulated by GHB and other compounds, suggesting a transporter-mediated saturable efflux process.

The toxicodynamic effect of GHB on respiration could be described with incorporation of this nonlinear brain uptake followed by a direct effect, as GHB-induced respiratory depression is due to a direct effect at $GABA_B$ receptors.

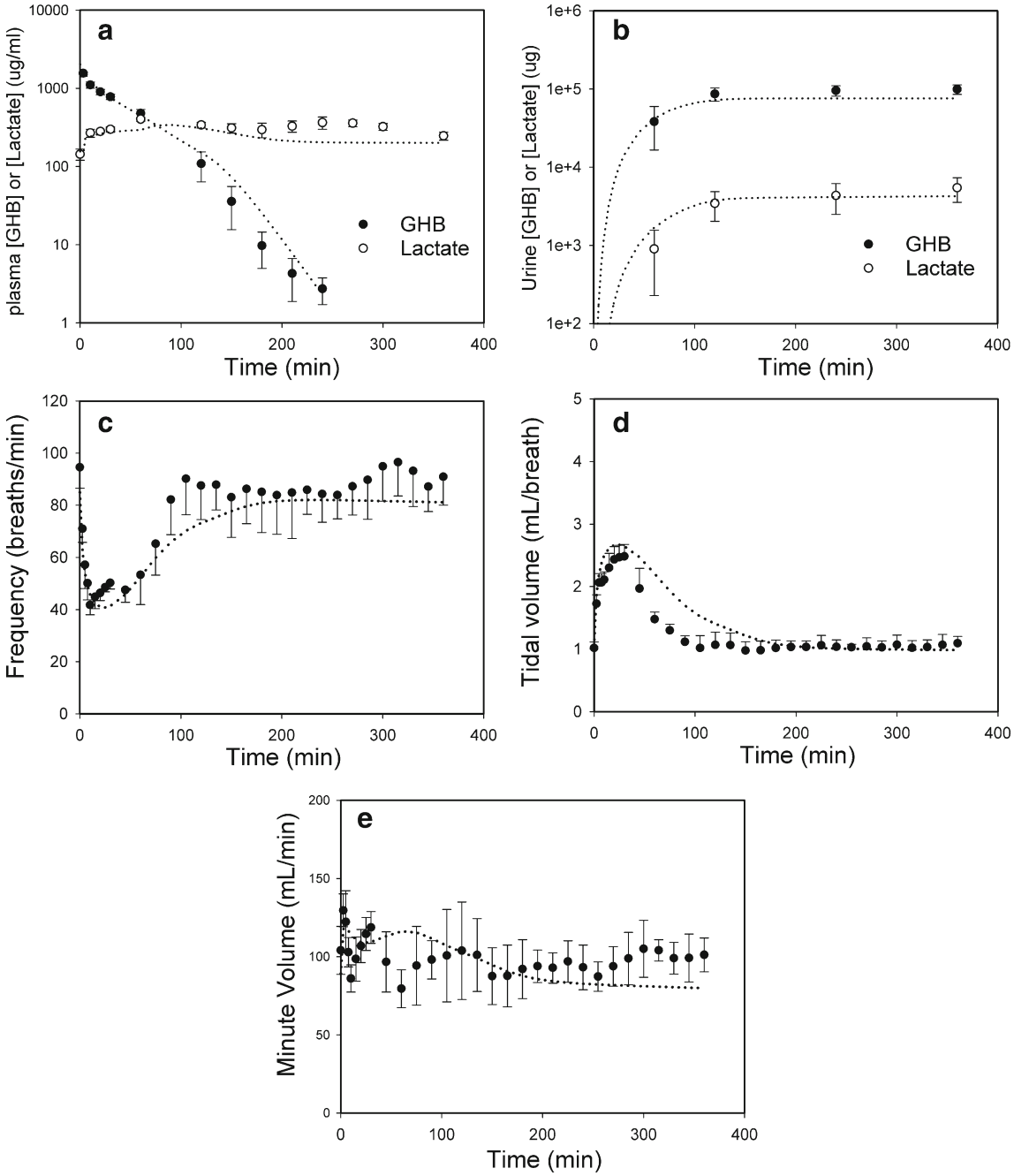


**Fig. 8.** Simulation of the model validation data. GHB 600 mg/kg was given intravenously at time 0. Intravenous sodium L-lactate 66 mg/kg+605 mg/kg/h was initiated 5 min later and continued for 8 h. **a** GHB and lactate plasma concentrations, **b** GHB and lactate urinary excretion, **c** breathing frequency, **d** tidal volume, **e** minute volume. *Symbols* represent experimental data presented as mean±SD and *dotted lines* those of the resulting simulations using the fitted model parameters

The effect of sodium L-lactate, however, was modeled with an indirect effect, as it is proposed that the metabolic alkalosis induced by exogenous sodium L-lactate infusion is responsible for effects of L-lactate on respiration since the metabolism of sodium L-lactate produces sodium bicarbonate, shifting acid–base balance in the blood (17). The function stimulating $k_{out}$ was used to model the increased use of hydrogen ions during this shift. This effect was not included for endogenous lactate since endogenous lactate is produced as lactic acid and, therefore, does not produce sodium bicarbonate upon its metabolism. The toxicodynamic results from sodium L-lactate infusion in this study suggest that while L-lactate may improve respiratory depression in GHB overdose by increasing GHB clearance, prolonged infusion may result in inhibition of respiratory depression at high lactate concentrations. Additionally, due to the observed toxicokinetic interaction of GHB decreasing lactate clearance, higher lactate concentrations than desired may be achieved with clinically relevant doses, and monitoring lactate concentrations may be warranted if used in clinical GHB overdose.

The primary limitation of the current model is that it describes the toxicokinetics of GHB following IV GHB administration, whereas in clinical overdose cases, GHB and its precursors are abused solely by oral ingestion. We and others have characterized the oral toxicokinetics of GHB in rats, which demonstrate a saturable oral absorption process, likely MCT-mediated, as well as saturable first-pass metabolism (8,13). While the TK/TD relationship should remain the same following IV or oral administration, for simulation of potential effects of GHB and MCT inhibitor administration in clinical GHB intoxication, the current TK/TD model needs to incorporate a physiologic oral absorption model. Furthermore, due to the involvement of MCTs in a number of GHB toxicokinetic parameters, the scale up of model parameters from rat to human will require quantitation of interspecies differences in transporter expression/activity, which is yet to be characterized at the physiologic sites of *in vivo* GHB transport.

## CONCLUSIONS

MCT-mediated transport governs the toxicokinetics of GHB and its interaction with L-lactate in many ways. Understanding of the MCT-mediated toxicokinetic processes for these two agents, incorporated into the current model, is necessary for understanding the potential value of L-lactate for the treatment of GHB overdose. The current model may be useful for the translation of this therapy in humans, following incorporation of a physiologic oral absorption model and *in vitro–in vivo* extrapolation of MCT-mediated processes.

## ACKNOWLEDGMENTS

This work was supported by the National Institutes of Health National Institute on Drug Abuse (grant DA023223).

## REFERENCES

1. Maitre M. The gamma-hydroxybutyrate signalling system in brain: organization and functional implications. Prog Neurobiol. 1997;51:337–61.
2. Caldicott DG, Chow FY, Burns BJ, Felgate PD, Byard RW. Fatalities associated with the use of gamma-hydroxybutyrate and its analogues in Australasia. Med J Aust. 2004;181:310–3.
3. Zvosec DL, Smith SW, Porrata T, Strobl AQ, Dyer JE. Case series of 226 gamma-hydroxybutyrate-associated deaths: lethal toxicity and trauma. Am J Emerg Med. 2011;29:319–32.
4. Liechti ME, Kupferschmidt H. Gamma-hydroxybutyrate (GHB) and gamma-butyrolactone (GBL): analysis of overdose cases reported to the Swiss Toxicological Information Centre. Swiss Med Wkly. 2004;134:534–7.
5. Wang Q, Darling IM, Morris ME. Transport of gamma-hydroxybutyrate in rat kidney membrane vesicles: role of monocarboxylate transporters. J Pharmacol Exp Ther. 2006;318:751–61.
6. Wang Q, Morris ME. The role of monocarboxylate transporter 2 and 4 in the transport of gamma-hydroxybutyric acid in mammalian cells. Drug Metab Dispos. 2007;35:1393–9.
7. Morris ME, Hu K, Wang Q. Renal clearance of gamma-hydroxybutyric acid in rats: increasing renal elimination as a detoxification strategy. J Pharmacol Exp Ther. 2005;313:1194–202.
8. Lettieri JT, Fung HL. Dose-dependent pharmacokinetics and hypnotic effects of sodium gamma-hydroxybutyrate in the rat. J Pharmacol Exp Ther. 1979;208:7–11.
9. Palatini P, Tedeschi L, Frison G, Padrini R, Zordan R, Orlando R, *et al*. Dose-dependent absorption and elimination of gamma-hydroxybutyric acid in healthy volunteers. Eur J Clin Pharmacol. 1993;45:353–6.
10. Bhattacharya I, Boje KM. GHB (gamma-hydroxybutyrate) carrier-mediated transport across the blood–brain barrier. J Pharmacol Exp Ther. 2004;311:92–8.
11. Roiko SA, Vijay N, Felmlee MA, Morris ME. Brain extracellular gamma-hydroxybutyrate concentrations are decreased by L-lactate in rats: role in the treatment of overdoses. Pharm Res. 2013;30:1338–48.
12. Lam WK, Felmlee MA, Morris ME. Monocarboxylate transporter-mediated transport of gamma-hydroxybutyric acid in human intestinal Caco-2 cells. Drug Metab Dispos. 2010;38:441–7.
13. Morse BL, Morris ME. Effects of monocarboxylate transporter inhibition on the oral toxicokinetics/toxicodynamics of gamma-hydroxybutyrate and gamma-butyrolactone. J Pharmacol Exp Ther. 2013;345:102–10.
14. Cui D, Morris ME. The drug of abuse gamma-hydroxybutyrate is a substrate for sodium-coupled monocarboxylate transporter (SMCT) 1 (SLC5A8): characterization of SMCT-mediated uptake and inhibition. Drug Metab Dispos. 2009;37:1404–10.
15. Morris ME, Morse BL, Baciewicz GJ, Tessena MM, Acquisto NM, Hutchinson DJ, *et al*. Monocarboxylate transporter inhibition with osmotic diuresis increases γ-hydroxybutyrate renal elimination in humans: a proof-of-concept study. J Clin Toxicol. 2011;1:1–4.
16. Morse BL, Vijay N, Morris ME. gamma-Hydroxybutyrate (GHB)-induced respiratory depression: combined receptor-transporter inhibition therapy for treatment in GHB overdose. Mol Pharmacol. 2012;82:226–35.
17. Tappy L, Cayeux MC, Chiolero R. Effects of sodium lactate on ventilation and acid–base balance in healthy humans. Clin Physiol. 1996;16:393–401.
18. Felmlee MA, Wang Q, Cui D, Roiko SA, Morris ME. Mechanistic toxicokinetic model for gamma-hydroxybutyric acid: inhibition of active renal reabsorption as a potential therapeutic strategy. AAPS J. 2010;12:407–16.
19. Raybon JJ, Boje KM. Pharmacokinetics and pharmacodynamics of gamma-hydroxybutyric acid during tolerance in rats: effects on extracellular dopamine. J Pharmacol Exp Ther. 2007;320:1252–60.
20. Dayneka NL, Garg V, Jusko WJ. Comparison of four basic models of indirect pharmacodynamic responses. J Pharmacokinet Biopharm. 1993;21:457–78.
21. Ishige K, Aizawa M, Ito Y, Fukuda H. gamma-Butyrolactone-induced absence-like seizures increase nuclear CRE- and AP-1 DNA-binding activities in mouse brain. Neuropharmacology. 1996;35:45–55.
22. Roiko SA, Felmlee MA, Morris ME. Brain uptake of the drug of abuse gamma-hydroxybutyric acid in rats. Drug Metab Dispos. 2012;40:212–8.
23. Tamai I, Takanaga H, Maeda H, Sai Y, Ogihara T, Higashida H, *et al*. Participation of a proton-cotransporter, MCT1, in the intestinal transport of monocarboxylic acids. Biochem Biophys Res Commun. 1995;214:482–9.
24. Ganapathy V, Thangaraju M, Gopal E, Martin PM, Itagaki S, Miyauchi S, *et al*. Sodium-coupled monocarboxylate transporters in normal tissues and in cancer. AAPS J. 2008;10:193–9.
25. Frank H, Groger N, Diener M, Becker C, Braun T, Boettger T. Lactaturia and loss of sodium-dependent lactate uptake in the colon of SLC5A8-deficient mice. J Biol Chem. 2008;283:24729–37.
26. Draoui N, Schicke O, Fernandes A, Drozak X, Nahra F, Dumont A, *et al*. Synthesis and pharmacological evaluation of carboxycoumarins as a new antitumor treatment targeting lactate transport in cancer cells. Bioorg Med Chem. 2013;21:7107–17.
27. Poole RC, Halestrap AP. Transport of lactate and other monocarboxylates across mammalian plasma membranes. Am J Physiol. 1993;264:C761–82.

28. Edlund GL, Halestrap AP. The kinetics of transport of lactate and pyruvate into rat hepatocytes. Evidence for the presence of a specific carrier similar to that in erythrocytes. Biochem J. 1988;249:117–26.
29. Metcalfe HK, Monson JP, Welch SG, Cohen RD. Inhibition of lactate removal by ketone bodies in rat liver. Evidence for a quantitatively important role of the plasma membrane lactate transporter in lactate metabolism. J Clin Invest. 1986;78:743–7.
30. Morse BL, Felmlee MA, Morris ME. gamma-Hydroxybutyrate blood/plasma partitioning: effect of physiologic pH on transport by monocarboxylate transporters. Drug Metab Dispos. 2012;40:64–9.
31. Kalvass JC, Polli JW, Bourdet DL, Feng B, Huang SM, Liu X, *et al*. Why clinical modulation of efflux transport at the human blood–brain barrier is unlikely: the ITC evidence-based position. Clin Pharmacol Ther. 2013;94:80–94.
32. Felmlee MA, Roiko SA, Morse BL, Morris ME. Concentration-effect relationships for the drug of abuse gamma-hydroxybutyric acid. J Pharmacol Exp Ther. 2010;333:761–71.